Published in final edited form as:
Nano Lett. 2010 November 10; 10(11): 4607–4613. doi:10.1021/nl102623x.

Coating Optimization of Superparamagnetic Iron Oxide Nanoparticles for High T_2 relaxivity

Sheng Tong[+], **Sijian Hou**[+], **Zhilan Zheng**, **Jun Zhou**, and **Gang Bao**[*]
Department of Biomedical Engineering, Georgia Institute of Technology and Emory University, Atlanta, GA 30332, USA.

Abstract

We describe a new method for coating superparamagnetic iron oxide nanoparticles (SPIOs) and demonstrate that, by fine-tuning the core size and PEG coating of SPIOs, the T_2 relaxivity per-particle can be increased by > 200 fold. With 14 nm core and PEG1000 coating, SPIOs can have T_2 relaxivity of 385 $s^{-1}mM^{-1}$, which is among the highest of all SPIOs reported. *In vivo* tumor imaging results demonstrated the potential of the SPIOs for clinical applications.

Keywords

SPIO; MRI contrast agent; nuclear relaxation; molecular imaging

Over the past two decades, superparamagnetic iron oxide nanoparticles (SPIOs) have received extensive studies as an important class of MRI contrast agent for medical imaging.[1, 2] A variety of SPIOs with different cores and surface coating were synthesized, and several are currently under clinical trials for imaging liver tumors and metastatic lymph nodes.[3–8] A SPIO, in general, is composed of maghemite or magnetite crystals less than 20 nm in diameter. Unlike widely used paramagnetic gadolinium chelates, these nanocrystals contain thousands of Fe atoms and approach saturation magnetization under a magnetic field typical for MRI.[9] Each nanocrystal can generate signal contrast several orders of magnitude higher than a gadolinium chelate. In addition, iron oxide has little toxicity for *in vivo* applications. These features make SPIOs an appealing candidate for early detection and diagnosis of atherosclerosis, cancer and many other human diseases. [6, 10–12]

SPIOs functionalized with specific targeting moieties can be used for *in vivo* imaging of molecular markers associated with disease development. For instance, imaging the SPIOs attached to VEGF receptors can help locate active tumors and determine tumor stages, since VEGF receptors are up-regulated on vascular endothelium involved in tumor angiogenesis, a process required for tumor expansion and metastasis.[13] However, molecular markers in small lesions usually present at a low level, which makes it very challenging for the SPIOs to generate a detectable contrast in MRI. Therefore, synthesizing SPIOs with substantial signal enhancement to improve sensitivity has been the most important issue in SPIO-based disease detection and diagnosis.

[*]Corresponding author: Tel: 1-404-385-0373. Fax: 1-404-894-4243. gang.bao@bme.gatech.edu.
[+]These authors contributed equally to this work.

Supporting Information Available: A complete description of the materials and methods used in experimentation are given, including details of the synthesis of iron oxide cores of different sizes, modeling of T_2 relaxivity of SPIOs, prediction of PEG coating layer thickness, stability of coated SPIOs in biological solutions, effects of functional groups and buffers on T_2 relaxivity, functionalization of SPIOs, and *in vivo* targeting of tumor with SPIOs. This material is available free of charge via the Internet at http://pubs.acs.org.

There are two major factors in determining the signal enhancement generated by the SPIOs: iron oxide core (size and material) and the coating (thickness and chemical composition). SPIOs can induce an increased T_2 relaxivity in MRI, which is determined by the translational diffusion of water molecules in the inhomogeneous magnetic field surrounding the SPIO.[14–16] Based on a quantum-mechanical outer-sphere theory, the T_2 relaxivity of SPIOs in solution can be given by (Supporting Information S1),[15, 16]

$$1/T_2=(256\pi^2\gamma^2/405)\, V^* M_s^2\, a^2/D\,(1+L/a) \quad (1)$$

where γ is the proton gyromagnetic ratio, V^*, M_s and a are the volume fraction, saturation magnetization and the radius of iron oxide core, respectively, D is the diffusivity of water molecules, and L is the thickness of an impermeable surface coating. For simplicity, only the secular term that dominates at high magnetic field is shown in Equation 1.[14] This theory predicts that the T_2 relaxivity of SPIOs increases with the magnetization and the size of iron oxide cores if the total amount of iron, V^*, is constant.[14, 17] Both mechanisms have been successfully explored with several experimental approaches. For example, the magnetization of SPIOs was enhanced by using cores formed by elementary iron or by doping iron oxide with other magnetic elements such as nickel, cobalt and manganese.[6, 18, 19] Further, the core size was increased by employing controllable crystallization through thermo-decomposition of iron complex in organic solvents.[4, 5, 19, 20] It has also been shown that the magnetization of magnetite increases with the crystal size at nanometer scale.[4,18]

The iron oxide core needs to be coated with either natural macromolecules or synthetic polymers in order to disperse in aqueous solutions.[4, 8, 21] In many cases, most of the magnetic field surrounding a SPIO falls within the coating. For instance, the magnetic field strength on the surface of a dextran-coated cross-linked iron oxide nanoparticle (CLIO) reduces to only 2.3% of that on the surface of its iron oxide core (The core radius and coating thickness of a CLIO are 4.35 nm and 10.8 nm, respectively.[22]). The coating molecules of a SPIO can exclude water from its surface, hinder water diffusion, or immobilize nearby water molecules by forming hydrogen bonds, all may affect the nuclear relaxation of water protons. Therefore, SPIOs synthesized with distinct coating schemes can exhibit significantly different T_2 relaxivity even if their iron oxide core sizes are similar. However, the effect of coating on T_2 relaxivity is not well understood.

A film hydration method has been used to coat nanocrystals with small amphiphilic molecules, such as poloxamer, poloxamine and phospholipid-PEG.[23] PEG is a hydrophilic polymer used extensively for improving blood circulation of liposomes and coating nanoparticles.[23–26] In the film hydration method, to produce micellar nanoparticles, the cores and coating molecules are dispersed in chloroform and deposited to a thin film after chloroform is evaporated. The outcome of this method, however, is controlled by a complicated interplay between three competing processes: formation of empty micelles, aggregation of nanocrystals and assembly of micellar nanoparticles. This often leads to low coating efficiency and wide size distribution of the SPIOs with a large amount of empty micelles and SPIO aggregates.

Here we report the development of a versatile coating method, combined with controllable core synthesis, to generate an array of water soluble SPIOs with different core sizes and coating thicknesses. We systematically studied the effects of core size and coating thickness of SPIOs on T_2 relaxivity, and optimized the composition of SPIOs for molecular imaging. Specifically, in this study, iron oxide cores were coated with 1, 2-distearoyl-sn-glycero-3-phosphoethanolamine-N-[methoxy (polyethylene glycol)] copolymer (DSPE-mPEG). To improve coating efficiency and size distribution of SPIOs, we developed a new solvent-

exchange method in which DSPE-PEG and iron oxide nanocrystals assemble in a solvent system with ascending solvent polarity. We found that high quality SPIOs can be generated consistently with this method. To our knowledge, this is the first demonstration that assembly of amphiphilic molecules on hydrophobic surface of a nanocrystal can be induced controllably by increasing the polarity of solvent systems with miscible solvents. This method is not only critical for the SPIO synthesis in the current study but may be extended to the assembly of amphiphilic molecules on different nanoparticle surfaces in general.

Iron oxide cores of two different sizes, 5 nm and 14 nm in diameter, were synthesized by solvent-free thermo-decomposition of iron complex using a procedure modified from a published method (Supporting Information, S2).[21] The as-synthesized cores are covered by oleic acid / oleylamine and dispersed in toluene. To form the coating, the iron oxide cores and DSPE-mPEG are initially dispersed in chloroform (Fig. 1a). The two components can be assembled into water soluble SPIOs by substituting chloroform with DSMO and water sequentially, which gradually increases polarity of the solvent system (Fig. 1b and 1c). In aqueous solutions, DSPE-mPEG is firmly attached to the iron oxide core through hydrophobic interaction between DSPE and oleic acid/oleylamine (Fig. 1d). We found that both 5 nm and 14 nm cores could be coated efficiently at room temperature by DSPE-mPEG with the molecular weight of PEG greater than 1000 Da. When the PEG size is smaller than 1000 Da, the coating procedure needs to be performed at 70°C. This is presumably due to the tendency of DSPE-mPEG to form lamellar structures, which can be circumvented by heating.[27] For comparison, we performed gel electrophoresis of the SPIOs synthesized with the film hydration method and the solvent exchange method respectively, and found that the solvent exchange method yielded better SPIOs with respect to the size and charge distribution (Supporting Information, S3).

The DSPE-mPEG coated SPIOs consist of an iron oxide core of 5 or 14 nm, a hydrophobic lipid bilayer and a water permeable PEG layer with variable PEG chain length (Figure 1d). The coated SPIOs exhibit narrow size distribution in water as determined by dynamic light scattering (Figure 1e). The measured hydrodynamic diameters of the 5 nm and 14 nm SPIOs with PEG1000 coating are 14.8±1.2 nm and 28.6±0.4 nm respectively, which are in good agreement with the theoretical predictions (14.56 nm and 23.74 nm, Supporting Information, S4). A thin and uniform layer of DSPE-mPEG coating is visible in negatively stained TEM images (insets of Fig. 1e). Note that the PEG1000 coating is considerably thinner than several PEG coatings developed elsewhere.[21, 28, 29] The coated SPIOs are stable in water, PBS and serum (Supporting Information, S5).

We measured the T_2 relaxivity (defined as $1/T_2$ normalized by molar concentration of Fe atoms) of the SPIOs with two core sizes (5 nm and 14 nm) and five PEG chain lengths (with molecular weights of 550, 750, 1000, 2000 and 5000 Da). As shown in Figure 2a, due to increased mass magnetization and core size, the 14 nm SPIOs consistently showed higher T_2 relaxivity than the 5 nm SPIOs with the same coating. The T_2 relaxivity of the 14 nm SPIOs increased by 2.54 fold when the PEG molecular weight decreased from 5000 to 1000 Da; however, it did not increase further when the PEG size further decreased to 750 Da and 550 Da. The change is even more significant for the 5 nm SPIOs; its T_2 relaxivity increased by 7.79 fold when PEG molecular weight decreased from 5000 Da to 550 Da. Interestingly, both cores have a critical PEG size, at which the T_2 relaxivity changed dramatically. With 14nm core and DSPE-PEG1000, SPIOs can have T_2 relaxivity of 385±39 s^{-1} mM^{-1}, which is among the highest per-Fe atom relaxivities of all SPIOs reported (Table 1).

The effect of PEG coating on the T_2 relaxivity can only be partly accounted for by the changes in the shell/core ratio, i.e., *L/a* in Equation 1, which assumes that the coating is impermeable (Fig 2c). For example, using the calculated PEG layer thicknesses (Supporting

Information, Table S2) and assuming the thickness of DSPE-oleic acid/oleylamine layer is 3 nm, Equation 1 predicts that the changes in T_2 relaxivity are only 1.66 and 1.97 fold respectively for the 14 nm and 5 nm SPIOs over the same PEG layer thickness range. This suggests that PEG molecules may immobilize water molecules in a region much larger than that predicted by Equation 1. Similarly, we found that surface functional groups and buffer conditions (pH value and ionic strength) could also change T_2 relaxivity, although to a much lesser degree (Supporting Information, S6).

To evaluate the detection sensitivity of the SPIOs as MRI contrast agents when the number of molecular targets is the limiting factor, we examined the T_2 relaxivity on a per particle basis (Fig. 2b). With DSPE-mPEG1000 coating, the T_2 relaxivity of the 14 nm SPIOs is 70 fold higher than that of the 5 nm SPIO. With the optimal combination of the core size and coating thickness, on a per particle basis, the T_2 relaxivity of the 14 nm SPIOs with PEG1000 is more than 200 fold higher than that of the 5 nm SPIOs with PEG5000.

The coating method developed in this study enables several strategies for conjugating targeting ligands as well as other functional moieties to the SPIOs. DSPE-PEG functionalized with small molecules, such as amine, maleimide, folic acid and biotin, can be mixed with DSPE-mPEG and coated on to the iron oxide cores at desired ratio. For example, the number of DSPE-mPEG2000-NH_2 per SPIO was found to be proportional to its initial loading ratio (Supporting Information, S7), with the maximum number of amine groups on each 14nm SPIO to be ~600. The DSPE-PEG-NH_2 coating density is in line with that of DSPE-mPEG2000 formed micelles.[27] In addition, coating the SPIO in liquid phase can facilitate an even distribution of functional groups among all nanoparticles, presumably due to rapid exchange between the DSPE-PEG coated on the nanoparticles and the monomeric DSPE-PEG in DMSO (Supporting Information, S3).[30] The mild transition condition of solvent exchange also allows the addition of sensitive functional groups such as maleimide to the SPIOs. This is advantageous compared with the traditional DSPE-PEG coating method, which requires extensive sonication and heating in aqueous solutions.[7, 23]

To demonstrate molecular targeting, SPIO-based detection was carried out in an *in vitro* assay mimicking an enzyme-linked immunosorbent assay (ELISA) (Figure 3). Specifically, DSPE-mPEG1000 is chosen as the surface coating based on T_2 relaxivity and coating efficiency measured, and the 5 nm and 14 nm SPIOs were conjugated with a goat anti-mouse-IgG antibody. To minimize steric hindrance of ligand binding, DSPE-PEG2000-maleimide was added to the SPIOs with DSPE-mPEG1000 coating, and the reduced antibodies were linked to the SPIO by thiol-maleimide reaction. A 96-well ELISA plate was coated with mouse IgG, ranging from 10 to 10^4 ng/mL, and saturated with bovine serum albumin (BSA). The mouse IgG loading was confirmed with a goat anti-mouse antibody conjugated with horseradish peroxidase (Fig. 3a). The wells were incubated with the conjugated SPIOs and the SPIOs bound in each well were quantified using a Ferrozine method (Fig. 3b). We found that the iron content of the bound SPIOs was proportional to protein loading within a wide range, from 1000 ng/ml down to 10 ng/ml (Fig. 3b), and the nonspecific binding between the SPIOs and BSA was negligible. With the same IgG loading concentration, the 14 nm SPIO had only a 10-fold increase in iron content compared with that of the 5 nm SPIO, lower than the 22-fold increase expected. This is likely due to the lower accessibility of the 14 nm SPIO to the protein targets on the plate surface. To further demonstrate the effect of bound SPIOs on T_2, wells containing SPIOs suspended in 50 μl of buffer with the equivalent amount of iron contents corresponding to that shown as Rows 1, 3, and 5 in Fig. 3b were imaged using a 7T small animal MRI instrument (Figs. 3c and 3d). The resulting images were used to construct a $1/T_2$ map (Fig. 3e). Our results demonstrate that the 14 nm SPIOs can bind to the target proteins specifically, with very high detection sensitivity.

To demonstrate the ability of detecting early-stage tumor using SPIOs as a contrast agent in MRI, we performed preliminary animal studies of *in vivo* tumor imaging with DSPE-PEG coated SPIOs, which exhibited longer blood circulation half-life (23.2 min) compared with other nanoparticles coated with DSPE-mPEG1000 (data not shown). Tumors were induced by implanting human U87 glioblastoma cells subcutaneously in nude mice. After the tumors reached 3~5 mm in diameter, the tumor-bearing mice were examined with a 7T MRI scanner before and one hour after tail vein injection of SPIOs conjugated with antibodies against mouse VEGF receptor-1. The specificity of VEGFR-1-targeting SPIOs was confirmed using an *in vitro* assay (Supporting Information, S8). As shown in Figure 4, injection of the 14 nm SPIOs resulted in a significant enhancement in T_2 contrast of the tumor tissue (Figs. 4c and 4e, and Supporting Information, S8).

In summary, we developed a novel method for coating and functionalizing superparamagnetic iron oxide nanoparticles using biocompatible DSPE-PEG copolymers through dual solvent exchange, and a new strategy for optimizing the signal contrast of SPIO-based probes, which have a great potential as an MRI contrast agents for clinical diagnostic imaging. We selected DSPE-PEG, a well-established biocompatible material for SPIO coating and optimization, since the immunogenicity and *in vivo* toxicity of a contrast agent and its metabolites are major issues in *in vivo* imaging applications.[31] Using the solvent-exchange method developed in our study, the DSPE-PEG coating is stable, versatile and offers an optimal shell/core ratio compared with many existing SPIOs (Table 1). We systematically quantified the dependence of T_2 relaxivity on the PEG layer thickness, and found that SPIOs with 14 nm core and DSPE-mPEG1000 coating provides the highest T_2 relaxivity on a per-Fe atom basis among all iron oxide nanoparticles reported. The T_2 relaxivity of the 14 nm SPIOs is even comparable to that of the manganese-doped iron oxide nanoparticles, which has demonstrated outstanding tumor detection sensitivity in mice.[6] More importantly, the high T_2 relaxivity was achieved by using well-recognized biocompatible materials for coating.[32] The 14 nm SPIOs are exceptional with respect to signal strength per particle and thus have the potential to provide a flexible platform for detecting molecular markers in low abundance in disease diagnostic imaging using MRI, as demonstrated by our preliminary studies of *in vivo* tumor detection.

Although the SPIOs synthesized in this work have excellent performance in terms of T_2 relaxivity and coating stability, their blood circulation half-life in mouse is relatively short (~23 min). This may be due to the non-specific uptake of cells in blood, including macrophages. Our solution study showed that 40–60 min is sufficient for antibody-conjugated SPIOs to bind to their target, which is consistent with the time required (~30 min) for antibody-antigen binding at 37°C. Although a quick removal of the SPIOs from the circulation may be beneficial for minimizing the background signal generated from unbound SPIOs, longer-circulating SPIOs may increase the chance of binding to the target molecules, thus an enhanced contrast. We found that the circulation half-life of the SPIOs increases with the PEG chain length (data not shown), and for certain SPIOs, adding free coating molecules to the SPIO solution injected can significantly prolong its blood circulation. Additional studies are being conducted on the circulation and bio-distribution of DSPE-PEG coated SPIOs to obtain a better understanding of their pharmacokinetics and the methods to modulate their bio-availability.

Supplementary Material

Refer to Web version on PubMed Central for supplementary material.

Acknowledgments

This work was supported by the National Institutes of Health as a Program of Excellence in Nanotechnology Award (HHSN268201000043C to GB), and as a Center of Cancer Nanotechnology Excellence Award (CA119338 to GB).

Reference

1. Wang YX, Hussain SM, Krestin GP. Eur Radiol. 2001; 11(11):2319–2331. [PubMed: 11702180]
2. Bjornerud A, Wendland MF, Johansson L, Ahlstrom HK, Higgins CB, Oksendal A. Acad Radiol. 1998; 5 Suppl 1:S223–S225. [PubMed: 9561086]
3. Weissleder R, Bogdanov A, Neuwelt EA, Papisov M. Advanced Drug Delivery Reviews. 1995; 16(2–3):321–334.
4. Jun YW, Huh YM, Choi JS, Lee JH, Song HT, Kim S, Yoon S, Kim KS, Shin JS, Suh JS, Cheon J. Journal of the American Chemical Society. 2005; 127(16):5732–5733. [PubMed: 15839639]
5. Xu CJ, Sun SH. Polymer International. 2007; 56(7):821–826.
6. Lee JH, Huh YM, Jun YW, Seo JW, Jang JT, Song HT, Kim S, Cho EJ, Yoon HG, Suh JS, Cheon J. Nat Med. 2007; 13(1):95–99. [PubMed: 17187073]
7. Nitin N, LaConte LE, Zurkiya O, Hu X, Bao G. J Biol Inorg Chem. 2004; 9(6):706–712. [PubMed: 15232722]
8. Yu WW, Chang E, Sayes CM, Drezek R, Colvin VL. Nanotechnology. 2006; 17(17):4483–4487.
9. Gossuin Y, Gillis P, Hocq A, Vuong QL, Roch A. Wiley Interdiscip Rev Nanomed Nanobiotechnol. 2009; 1(3):299–310. [PubMed: 20049798]
10. Nahrendorf M, Jaffer FA, Kelly KA, Sosnovik DE, Aikawa E, Libby P, Weissleder R. Circulation. 2006; 114(14):1504–1511. [PubMed: 17000904]
11. Montet X, Montet-Abou K, Reynolds F, Weissleder R, Josephson L. Neoplasia. 2006; 8(3):214–222. [PubMed: 16611415]
12. Winter PM, Morawski AM, Caruthers SD, Fuhrhop RW, Zhang H, Williams TA, Allen JS, Lacy EK, Robertson JD, Lanza GM, Wickline SA. Circulation. 2003; 108(18):2270–2274. [PubMed: 14557370]
13. Carmeliet P. Nat Med. 2003; 9(6):653–660. [PubMed: 12778163]
14. Gillis P, Koenig SH. Magn Reson Med. 1987; 5(4):323–345. [PubMed: 2824967]
15. Gillis P, Moiny F, Brooks RA. Magn Reson Med. 2002; 47(2):257–263. [PubMed: 11810668]
16. Brooks RA, Moiny F, Gillis P. Magn Reson Med. 2001; 45(6):1014–1020. [PubMed: 11378879]
17. Koenig SH, Kellar KE. Magn Reson Med. 1995; 34(2):227–233. [PubMed: 7476082]
18. Jun YW, Seo JW, Cheon A. Accounts of Chemical Research. 2008; 41(2):179–189. [PubMed: 18281944]
19. Tromsdorf UI, Bigall NC, Kaul MG, Bruns OT, Nikolic MS, Mollwitz B, Sperling RA, Reimer R, Hohenberg H, Parak WJ, Forster S, Beisiegel U, Adam G, Weller H. Nano Letters. 2007; 7(8): 2422–2427. [PubMed: 17658761]
20. Yu WW, Falkner JC, Yavuz CT, Colvin VL. Chemical Communications. 2004; (20):2306–2307. [PubMed: 15489993]
21. Xie J, Xu C, Kohler N, Hou Y, Sun S. Advanced Materials. 2007; 19(20):3163–3166.
22. Reynolds F, O'Loughlin T, Weissleder R, Josephson L. Analytical Chemistry. 2005; 77(3):814–817. [PubMed: 15679348]
23. Dubertret B, Skourides P, Norris DJ, Noireaux V, Brivanlou AH, Libchaber A. Science. 2002; 298(5599):1759–1762. [PubMed: 12459582]
24. Torchilin VP. Nat Rev Drug Discov. 2005; 4(2):145–160. [PubMed: 15688077]
25. Sperling RA, Pellegrino T, Li JK, Chang WH, Parak WJ. Advanced Functional Materials. 2006; 16:943–948.
26. Yu WW, Chang E, Falkner JC, Zhang J, Al-Somali AM, Sayes CM, Johns J, Drezek R, Colvin VL. J. Am. Chem. Soc. 2007; 129:2871–2879. [PubMed: 17309256]
27. Johnsson M, Hansson P, Edwards K. Journal of Physical Chemistry B. 2001; 105(35):8420–8430.

28. Kohler N, Sun C, Fichtenholtz A, Gunn J, Fang C, Zhang MQ. Small. 2006; 2(6):785–792. [PubMed: 17193123]
29. Gupta AK, Curtis AS. J Mater Sci Mater Med. 2004; 15(4):493–496. [PubMed: 15332623]
30. Wang YM, Kausch CM, Chun MS, Quirk RP, Mattice WL. Macromolecules. 1995; 28(4):904–911.
31. Weissleder R, Stark DD, Engelstad BL, Bacon BR, Compton CC, White DL, Jacobs P, Lewis J. Am J Roentgenol. 1989; 152:167–173. [PubMed: 2783272]
32. Weissleder R, Elizondo G, Wittenberg J, Rabito CA, Bengele HH, Josephson L. Radiology. 1990; 175(2):489–493. [PubMed: 2326474]
33. Lee H, Yu MK, Park S, Moon S, Min JJ, Jeong YY, Kang HW, Jon S. J Am Chem Soc. 2007; 129(42):12739–12745. [PubMed: 17892287]
34. Koenig SH, Kellar KE, Fujii DK, Gunther WH, Briley-Saebo K, Spiller M. Acad Radiol. 2002; 9 Suppl 1:S5–S10. [PubMed: 12019893]

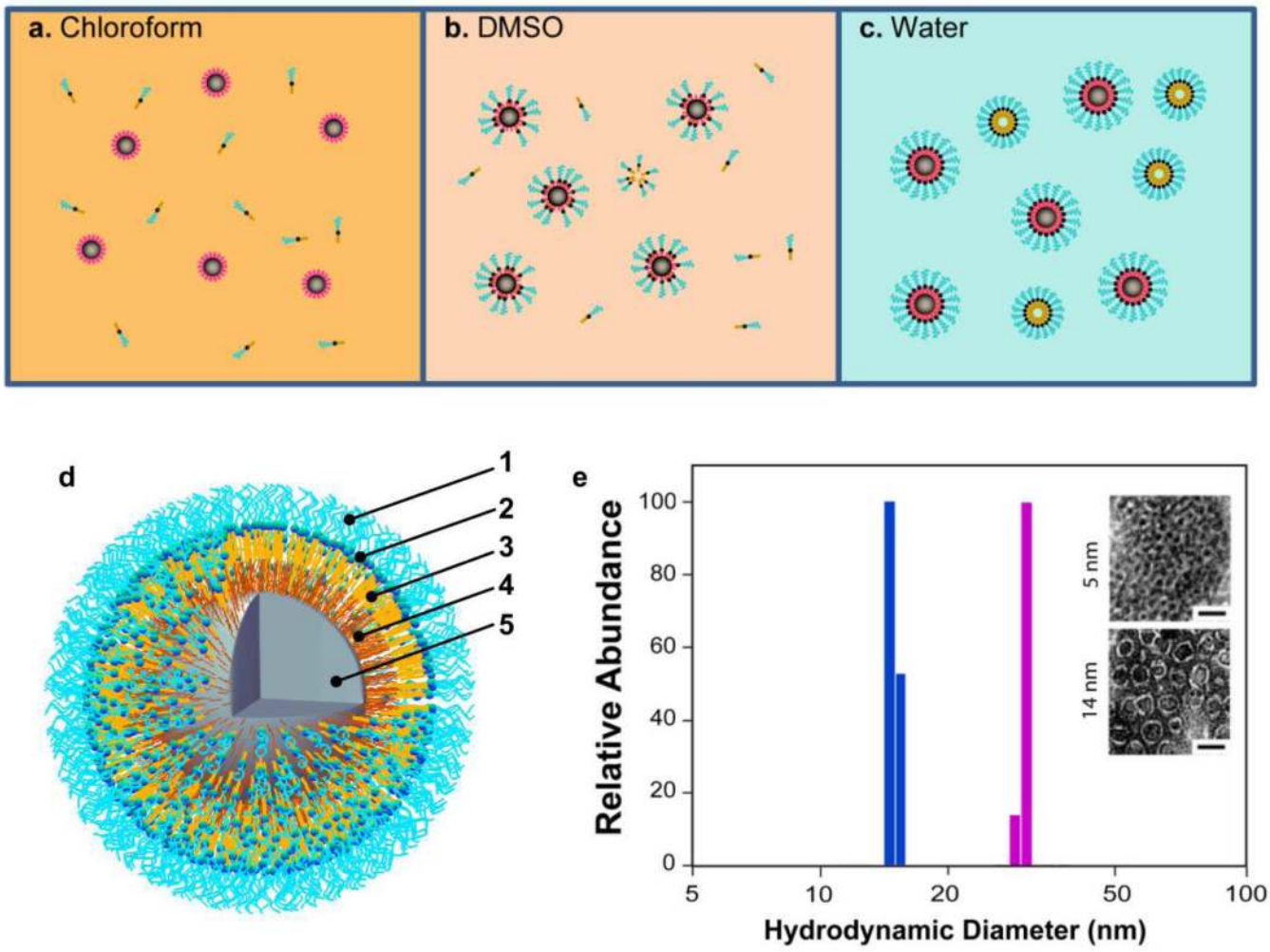

Figure 1. A schematic diagram of SPIO synthesis and coating schemes

a. Both iron oxide cores and DSPE-PEG are dissolved in chloroform. **b.** Addition of DMSO induces assembly between iron oxide cores and DSPE-PEG molecules. **c.** Transition into water further strengthens the hydrophobic interaction between DSPE-PEG and oleic acid/ oleylamine on iron oxide cores. Due to its extremely low CMC (~5μM in water), unoccupied DSPE-PEG exists mainly in the form of empty micelles. **d**. A schematic diagram of a SPIO with 4.8nm iron oxide core and DSPE-mPEG1000 coating. **1** through **5** represent PEG, phosphate, DSPE, oleic acid / oleylamine and the iron oxide core, respectively. The dimensions are based on TEM measurement and numerical analysis (supplementary information, SII & SIII). **e.** Dynamic light scattering of the SPIOs coated with DSPE-mPEG1000. Blue: Number-weighted size distribution of 5nm iron oxide core coated with DSPE-mPEG1000, average size = 14.8±1.2 nm. Purple: 14 nm iron oxide core coated with DSPE-mPEG1000, average size = 28.6±0.4 nm. Shown in the inset are TEM images of iron oxide cores and coated SPIOs negatively stained with phosphotungsic acid to give a white layer surrounding the iron oxide cores indicating the DSPE-mPEG1000 coating layer.

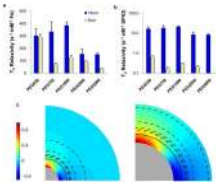

Figure 2. Dependency of T_2 relaxivity on the core size and the PEG chain length of the SPIOs

a. T_2 relaxivity of the SPIOs with constant iron concentration. **b**. T_2 relaxivity of the SPIOs on a per particle basis. SPIOs with two core sizes, 5nm and 14nm, and five PEG sizes, molecular weight of 550, 750, 1000, 2000 and 5000 Da, were evaluated. **c**. Normalized magnetic field of the two iron oxide cores (Left: 5nm & Right 14nm). The color bar represents the magnitude of the magnetic field strength (z-component) of the iron oxide cores. The magnetic field strength is normalized by its value at the equator line on the core surface. Solid line and dashed lines represent the boundaries of lipid bilayer and PEG coating layers, respectively. Starting from the centre, the dash lines indicate PEG550, PEG750, PEG1000, PEG2000 and PEG5000.

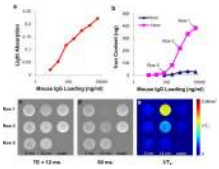

Figure 3. ***In vitro*** **targeting**

A 96-well ELISA plates were coated with mouse IgG at designated protein loading concentration. The wells coated with mouse IgG was incubated with either antibody conjugated horseradish peroxidase or the SPIOs at 37°C for 1 hour. **a**. Wells were incubated with goat anti-mouse IgG conjugated with horseradish peroxidase. Horseradish peroxidase activity was detected by ABTS. **b**. Wells was incubated with SPIOs conjugated with goat anti mouse IgG. Iron content of bound SPIOs was measured using Ferrozine method. **c** and **d**. The plate was loaded with designated amount of 5nm or 14nm SPIOs suspended in 50μl of water and imaged with a 7T MRI instrument using spin-echo sequence with echo time equal to 12ms and 60ms, respectively. **e**. T_2 effect calculated based on MRI images.

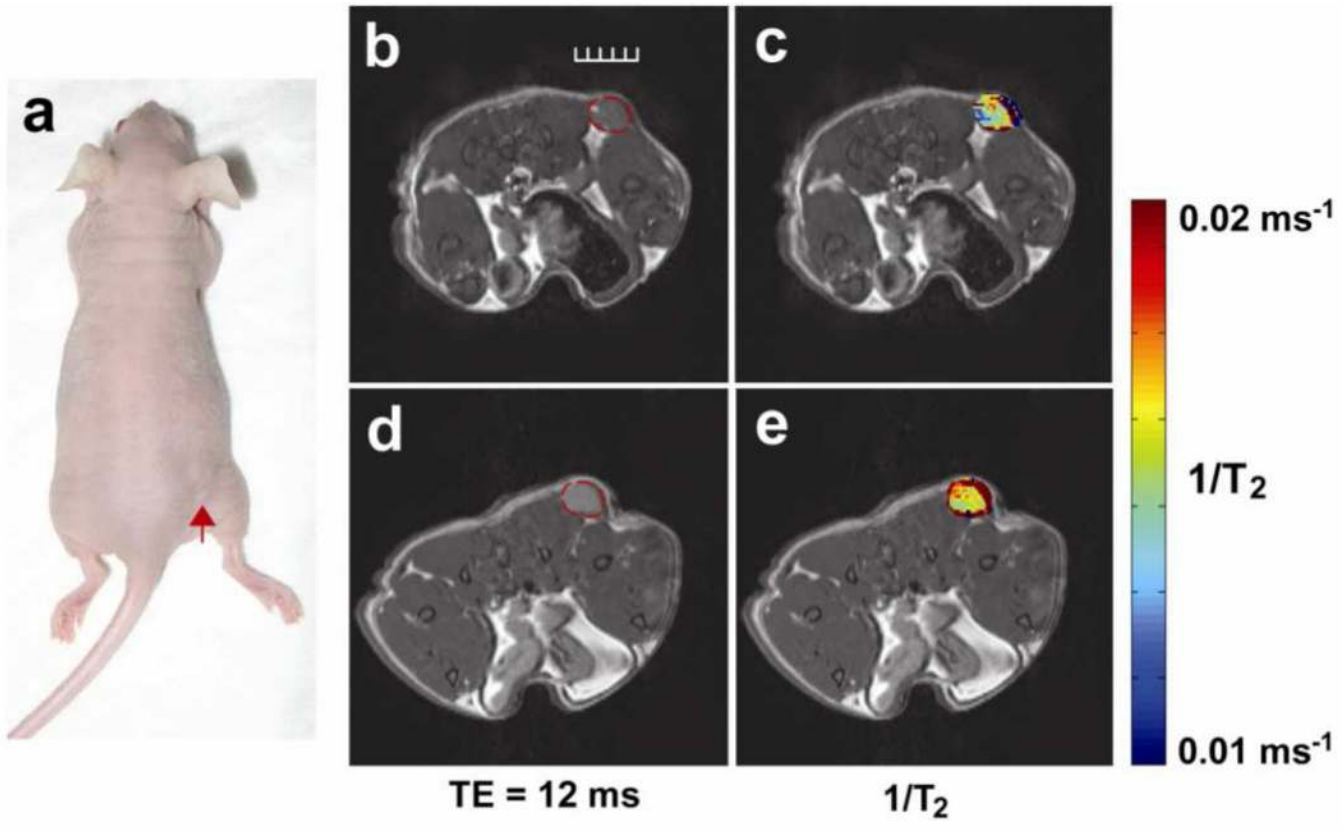

Figure 4. ***In vivo*** **tumor imaging**

MRI experiments were performed using spin-echo sequence. **a**. Arrow shows the location of the subcutaneous tumor. **b** and **c**. MR images of tumor before probe injection. **d** and **e**. MR images collected after 1 hour following the injection of 14nm SPIOs conjugated with antibodies against mouse VEGFR-1. Red dotted lines in **b** and **d** outline the tumor. Scale bar represents 5 mm.

Table 1

Relaxivities, core and hydrodynamic sizes of Different SPIOs

SPIOs	Coating	Core size (nm)	Hydrodynamic Diameter (nm)	T_2 relaxivity ($s^{-1}mM^{-1}$)
SPIO-14	DSPE-mPEG1000	13.8	28.6 ± 0.4	385± 39
SPIO-5	DSPE-mPEG1000	4.8	14.8 ± 1.2	130 ± 5
SPIO-12[4]	DMSA	12	-	218
SPIO-7[33]	poly(TMSMA-r-PEGMAr-NAS)	3–10	25.6 ± 2.7	-
SPIO-9[21]	DPA-PEG600	9	40	-
CLIO [11, 22]	Cross-linked dextran	8.74 ± 3.09	28 ± 3.1	111 ± 1
MION-46®[34]	Dextran	8.05	21.9	43.7
Clariscan®[2, 34]	Carbohydrate-PEG	6.43	11.9	35.0